

Concerted regulation of all hyphal tips generates fungal fruit body structures: experiments with computer visualizations produced by a new mathematical model of hyphal growth

Audrius MEŠKAUSKAS, Liam J. McNULTY and David MOORE*

*School of Biological Sciences, Stopford Building, University of Manchester, Oxford Road, Manchester M13 9PT, UK.
E-mail: david.moore@man.ac.uk*

Received 10 December 2003; accepted 12 January 2004.

Filamentous hyphal growth is inherently suited to kinetic analysis, and in many respects the fungal mycelium can be viewed as a very mechanical biological system, which lends itself to mathematical modelling. The mathematics of hyphal tip extension growth are well-established. However, even though a hyphal growth equation can be written with confidence, and we have a good understanding of the effects of tropisms on growth, it is not easy to form a mental picture of the behaviour of large populations of hyphal tips. What is required, and what we believe we have produced, is a mathematical model that is sufficiently sophisticated to produce a realistic visualization of fungal hyphal growth. This provides us with a cyberfungus that can be used for experimentation on the theoretical rules that might govern hyphal patterning, hyphal interactions, and tissue formation and organ development by actually visualizing the virtual hyphal growth patterns that result from different regulatory scenarios. From a series of model experiments the most significant observation is that complex fungal fruit body shapes can be simulated by applying the same regulatory functions to all of the growth points active in a structure at any specific time. No global control of fruit body geometry is necessary. No localized regulation is necessary. The shape of the fruit body emerges from the concerted response of the entire population of hyphal tips, in the same way, to the same signals.

INTRODUCTION

Direct observation and measurement of the growth of filamentous fungi has established a number of general relationships that are expressed in equation (1) (Steele & Trinci 1975, Trinci 1984, Trinci *et al.* 1994):

$$\bar{E} = \mu_{\max} G \quad (1)$$

where \bar{E} is the observed mean rate of extension growth at the tip, μ_{\max} is the maximum specific growth rate, and G is the hyphal growth unit. G is defined as the average length of a hypha supporting a growing tip according to the so-called Trinci equation (2):

$$G = \frac{L_t}{N_t} \quad (2)$$

L_t being total mycelial length and N_t the number of hyphal tips (= number of branches). The hyphal growth unit is approximately equal to the width of the peripheral growth zone (more accurately, the volume of the hyphae within that zone), which is a ring-shaped

peripheral area of the mycelium that contributes to radial expansion of the colony. It is clearly evident that equation (1) contains most of the elements necessary to define hyphal morphology – hyphal length, number of branches and growth rate (Pirt 1967, Trinci 1971, 1984, Prosser & Trinci 1979, Trinci *et al.* 1994). It lacks any definition of growth direction and branch patterning, causative, analytical and descriptive aspects of which have been discussed by several authors in recent years (Obert, Pfeifer & Sernetz 1990, Ritz & Crawford 1990, Yang *et al.* 1992, Matsuura & Miyazima 1993, Viniegra-Gonzalez *et al.* 1993, Momany 2002, Olsson 2002, Ott *et al.* 2003). The influence of external factors on the direction of hyphal growth and branching is obviously relevant to any attempt at computer visualization of hyphal growth. External effectors can cause tropisms, which are evidenced as growth towards (+ve tropism) or away from (–ve tropism) the source of the ‘signal’. Growing hyphae appear actively to avoid each other, a negative autotropism (Robinson 1973a, b, Trinci *et al.* 1979, Hutchinson *et al.* 1980), but fungi exhibit a variety of tropic reactions in response to gravity, light, chemicals and some other external stimuli (Robinson 1973a, Moore 1991), including galvanotropism (Lever

* Corresponding author.

et al. 1994). Most of these phenomena are well enough understood to be incorporated into a mathematical model, providing due attention is paid to the nature of the signal, its propagation through the medium, and its attenuation (e.g. gravity pervades all of space and cannot be shaded and does not attenuate over biological distances, electromagnetic radiation can be shaded and may be absorbed or reflected and attenuation follows the inverse square law, chemicals will diffuse, and may lose (by decay) or gain (by activation) potency during diffusion, according to their individual physical and chemical characteristics). It is important to recognise that a mathematical model will deal with these features as abstractions; their reality may require experimental proof, but the need for, and nature of, the experiment may be suggested by the abstract model. We will emphasize this in the descriptions that follow because although it is often useful shorthand to refer to a specific tropism by name, the visualizations result from the abstract mathematical treatment of physical parameters. Consequently, our inclusion of a specific tropism in a description should not be taken as a prediction for the involvement of that specific signal, but should be understood to stand for a signal of similar physical parameters.

We have brought together the various features mentioned above and developed a vector-based mathematical model in which the growth vector of each virtual hyphal tip depends upon values derived from its surrounding virtual mycelium at each iteration of the algorithm. Effectively the virtual hyphal tip is sensing the neighbouring mycelium, which is why we call it the Neighbour-Sensing model. Obviously, the computation load increases with increase in the number of hyphal tips the model creates. However, the basic model remains within the scope of current desktop personal computers and an interactive version of the basic model can be found at <http://www.world-of-fungi.org/Models/index.htm>.

MATERIALS AND METHODS

Mathematical description of the model

Data representation

Each point and each growth vector contains three components, labelled in this description as p_x , p_y and p_z . The elementary unit in the latest version of the model is the hyphal section, defined as a part of the mycelium without branches. The section starts at the branch point of the parent section and ends either with the growing tip or (if the section has branched) with the next branch point. The data structure used to describe the section S contains information about the start point (S_{from}), end point (S_{to}), the growth vector S_{growth} , and a list of the daughter sections (S_{branches}). As a result of the alterations of the growth direction in response to tropic stimuli the section usually has the form of some

sort of curve rather than a straight line. To support this, most of the sections also contain a list of internal points ($S_{\text{subsegments}}$). We define n as the total number of sections in the mycelium at the given time t , and Y_i ($i \in [1 \dots n]$) as the list of sections in the mycelium at time t .

Field concept

Tropisms and branching regulation are implemented using the field concept. It is supposed that each point of the mycelium generates two types of field. The first type is used to implement a short distance hyphal avoidance reaction and to regulate branching. As the field is generated by all points of the mycelium, it is necessary to find a list of points S_A (size $S_{A_{p_n}}$). This list must be sufficiently large that the averaged field of all its members would be approximately equal to the field of the section. Then the field of the section at the arbitrary point p is:

$$N_{S,p} = \frac{l_c}{S_{A_{p_n}}} \sum_{j=1}^{S_{A_{p_n}}} \frac{1}{|S_{A_p} - p|^2} \quad (3)$$

To compute S_{A_p} , the list $\{S_{\text{from}}\} \cup S_{\text{subsegments}} \cup \{S_{\text{to}}\}$ is converted into the list of geometrical sections L , where each section connects two adjacent points. The field of each geometrical section is computed as the averaged field of m equally dispersed points (making set $P(m)$). The algorithm exponentially increases m until the field, computed by dividing the section into m points does not differ from the field computed by dividing it into $m-1$ points by more than the tolerance value ϵ . After the appropriate m is found, all points from $P(m)$ are added to S_{A_p} . As can be seen from equation (3), the value of this field is inversely proportional to the square of the distance to the point generating the field. This is true for physical fields such as the electrical or gravitational fields. Parameter l_c is the additional adjustment constant, making parameter sets compatible with older model versions, where the field was generated only by hyphal tips and branch points. The total field of the mycelium for the point of interest p is then equal to:

$$N_p = \sum_{\forall S: (S \in Y) \cdot (p \notin S)} N_{S,p} \quad (4)$$

In other words, we suppose that the hyphal section is unable to sense its own field as this would otherwise contribute an infinite value due to it having zero distance.

Another type of field ($M_{S,p}$) is responsible for the long-range interaction. The program allows us to choose between two options:

$$M_{S,p} = \frac{l_c}{S_{A_{p_n}}} \sum_{j=1}^{S_{A_{p_n}}} \frac{1}{\sqrt{|S_{A_p} - p|}} \quad (5)$$

or

$$M_{S,p} = \frac{I_c}{S_{A_{p_n}}} \sum_{j=1}^{S_{A_{p_n}}} \sqrt{|S_{A_p} - p|} \quad (6)$$

Equation (6) supposes that the field has a stronger value for more remote objects. This may look unusual to the physicist, but it is possible if the biological field is in reality caused by some chemical substance that changes as it diffuses. For example, if such a substance is released in an inactive form and slowly changes into an active form while it diffuses, the remote sources may have stronger impact than the immediate surroundings. The formula for the total field of the mycelium is identical to equation (4):

$$M_p = I_m \sum_{\forall S: (S \in Y) \cdot (p \notin S)} M_{S,p} \quad (7)$$

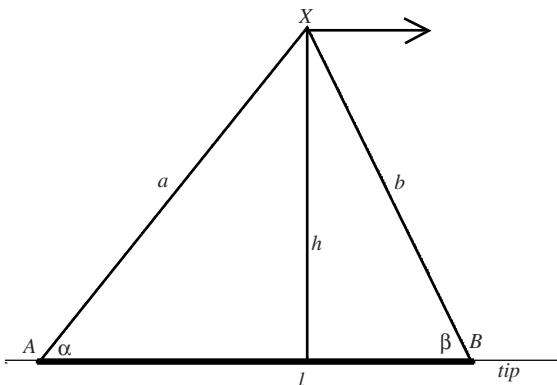
Here, I_m is the impact factor of the long distance autotropic reaction.

A third type of autotropic interaction is inversely proportional to the sixth degree of the distance. Such an interaction will decline very rapidly, but by setting the impact factor higher it is possible to have interaction at a particular distance. Bringing this factor into operation enables circling of one hypha around another. The formula for this field (8) is similar to formulas of the hyphal density field and the secondary autotropic field:

$$Q_{S,p} = \frac{I_c}{S_{A_{p_n}}} \sum_{j=1}^{S_{A_{p_n}}} \frac{1}{\sqrt{|S_{A_p} - p|^6}} \quad (8)$$

The galvanotropic field

Hyphal segments short enough to be considered as straight lines, form the galvanotropic orientation field. This field is directed toward the end of the segment that is closer to the corresponding hyphal tip and is parallel to the hyphal axis (see figure below). The absolute value of the field at any given point is inversely proportional to the shortest distance from that point to the segment generating the field. The total field of the mycelium at any given point is a vector sum of all the fields generated by all such mycelial segments.



The field is generated using the following rules:

- It is zero if $\alpha > 90^\circ$ or $\beta > 90^\circ$ (this means that $[-\frac{b^2 - a^2 - l^2}{al} < 0] + [-\frac{a^2 - b^2 - l^2}{bl} < 0]$).
- Otherwise, it is parallel to the hyphal axis l and is directed toward the apical end of the section (equation 9):

$$v_c = \frac{1}{h^2} \cdot \frac{B-A}{l} = \frac{1}{\left(\frac{1}{2}a\sqrt{4 - \frac{(b^2 - a^2 - l^2)^2}{a^2l^2}}\right)^2} \cdot \frac{B-A}{l} \quad (9)$$

After assuming this field it is possible to introduce two new types of tropism. The first is a parallel tropism that directs the growing hyphae to turn into the same direction of growth. The second orients hyphae perpendicularly to v_c , and can be used as a specific replacement of the previously mentioned positive and negative autotropisms:

$$v_d = \text{norm} \left(\begin{bmatrix} p(0, l, A_1, B_1, k) \\ p(0, l, A_2, B_2, k) \\ p(0, l, A_3, B_3, k) \end{bmatrix} - X \right) \quad (10)$$

where

$$k = a \cdot \cos \alpha = -\frac{b^2 - a^2 - l^2}{l}$$

$$p(x_a, x_b, y_a, y_b, x) = \frac{y_a - y_b}{x_a - x_b} (x - x_a) + y_b$$

and

$$\text{norm}(v) = \frac{v}{|v|}$$

Finally, to produce polarized structures, like mushroom fruit bodies, we introduced the concept of the orientation field. In contrast to the previous fields, this is a directional field, oriented in the direction of the z axis. The hyphae can try to grow by any arbitrary chosen angle $\beta \in [0 \dots 180^\circ]$ in relation to the vector of this field.

Growth simulation

Fields, defined by equations (3), (6) and (9) are scalar, and growth can be directed towards or against their gradient. All these equations can be differentiated with respect to p_x , p_y and p_z , obtaining the values for the field gradient vector at the point p (we used the program 'Maplesoft Maple' for differentiation and code generation). If several field concepts are used, we obtain several field gradients. To facilitate analysis, the gradient vectors can be displayed next to the growing

hyphal tips. Then, the current orientation of the cumulative tropism vector for the section S is:

$$v_S = \frac{dN_{S_{to}}}{dS_{to}} + \frac{dM_{S_{to}}}{dS_{to}} + \frac{dO_{S_{to}}}{dS_{to}} + I_g g(S, \beta) + I_c v_c + I_D v_D \quad (11)$$

where I_c and I_d define the impact factors of the parallel and positive/negative galvanotropisms, and:

$$g(S, \beta) = \begin{bmatrix} 0 \\ 0 \\ \Psi(|\beta - \text{angle}(S)| - \beta_{\text{tolerance}}) \text{sgn}(\beta - \text{angle}(S)) \end{bmatrix} \quad (12)$$

Here, differentiation with respect to the point $p = S_{to}$ means differentiation with relation to p_x for the vector component x , etc. The function g defines the impact of the orientation field and the model parameter I_g – the impact of this tropism on the orientation and $\text{angle}(S)$ is the tip orientation angle for the section S . Equation (12) incorporates a tolerance angle $\beta_{\text{tolerance}}$ to avoid the tip hunting around the optimum.

The growth vector of the section is updated in the following way:

$$S_{\text{growth}}^{\text{new}} = \text{norm}[k \cdot S_{\text{growth}} + (1 - k) \cdot \text{norm}(v_s)] \quad (13)$$

$$\text{where } \text{norm}(x) = \frac{x}{|x|}.$$

In equation (13), the parameter k defines a coefficient of persistence, which is used to ensure that branches change direction gradually; and it operates on the previous growth vector S_{growth} . The function $\text{norm}(x)$ ensures that the density gradient alters the direction but not the speed of the growth. Otherwise, a high gradient, if formed accidentally, would cause unreliably fast growth in some parts of the mycelium. The position of the tip is updated, the new value being equal to $S_{to}^{\text{new}} = S_{to} + a \cdot S_{\text{growth}}$, where a is the model parameter, defining the growth rate. In the current version of the model, growth is only possible if the hyphal section is terminated with an unbranched hyphal tip.

Vector rotation

Interesting results can be obtained if the tropism vectors $\frac{dN_{S_{to}}}{dS_{to}}$ and $g(S, \beta)$ are rotated around the hyphal axis before using them for modification of the growth vector. The model allows rotation of these vectors by an arbitrary angle, applying the known formulas for vector rotation. Rotation of the vector of the autotropic reaction can cause curling of the growing tip around the other hyphae. Rotation of the gravitropic vector may form spiral structures inside the mycelium.

Branching

In our model branch initiation is controlled by two steps. In the first step, the branching condition is checked. Depending on the experimenter's choice this condition can be

$$N_{S_{to}} < N_{\text{branch}} \text{ or } \sum_{\forall \Omega: \Omega \in Y} (\Psi(R - |S_{to} - \Omega_{to}|)) < N_{\text{branch}}$$

N_{branch} is the model parameter, defining either the number of neighbouring tips in the sphere of radius R or the threshold value of the density field.

In the next step, a random uniformly distributed number $r \in [0 \dots 100]$ is generated and branching is initiated if $r < p_{\text{branch}}$. The parameter p_{branch} defines the branching probability during one iteration if the initial branching condition is satisfied.

Formally the section branches into two, but one of the branches (the primary) assumes a copy of the growth vector of the parent branch, and continues in the same direction. Depending on the user-modifiable settings, the other (secondary) branch can be oriented randomly or adjusted to follow the direction of the tropic vector at the point of branching. S_{from} and S_{to} values of new branches are initialized to the S_{to} value of the parent branch.

Age and length limitations

Branching conditions can be extended, allowing branching only for sections whose ages do not exceed the given limit. Similarly, it is possible to set age and length limits for branch growth. To implement these features, each section contains two additional fields, S_{age} and S_{length} . During each iteration S_{age} is incremented by 1 and S_{length} is incremented by a .

Parallel processing

The program allows simulation of the development of small mycelia interactively, using a modest desktop or laptop PC. For larger structures like fungal fruit bodies the speed of single-processor computers is not sufficient. As each of several hundreds of hyphal tips is driven by exactly the same algorithm, the task is ideal for parallel execution and this has been implemented in the program, enabling use of several processors and longer running times. At the time of writing we are gathering experience in use of the program with multi-processor machines in Manchester Computing's High Performance Computer (HPC) unit. So-called 'supercomputers' usually require the tasks to be submitted in batch mode where interactive dialogue with the user is not possible. To partially compensate for this the program stores the generated mycelia in XML files (see below), which can be opened by a PC running the program to view the generated shapes. If needed, the user can modify some parameters and then continue the simulation by resubmitting the XML file to the supercomputer with altered parameter sets. Implementation in Java allows

the same program to be run on different computer types.

Describing mycelia and parameters in XML

Data definition in XML language consists of multiple tags, each having a name, associated parameters and possibly other, nested tags. As the tags can be accessed by name, introducing new tags does not make the previously stored data files incompatible as long as the default values of these new tags are known. Hence XML is a good language for defining the model parameters, as the number of parameters rapidly increases during program development. We also used the same XML file to store details about all placed substrates and all sections of mycelium. When the parameter tags only occur once per file, the <section> tag is repeated for each section of mycelium, and the <substrate> tag is repeated for each substrate. Such combined parameter-data files can be created on a desktop PC and later started on a supercomputer. Supercomputers generate the analogous XML file that can then be reloaded to the desktop PC for viewing the results, modifying some parameters and possibly returning to the supercomputer for further continuation. Being human-readable, XML also allows the experimenter to see the exact definitions of each section of mycelium.

Non-mathematical description of the Neighbour-Sensing model

The essential element of the Neighbour-Sensing model is a hyphal tip that has position in three-dimensional space, has a growth vector and has length, and an ability to branch. During each iteration of the algorithm the tip advances by a growth vector (initially set by the user) in accordance with the effects of one or more tropic vectors, and may branch (with an initial probability set by the user), also in accordance with the effects of one or more tropisms set by the user. The program has a user-friendly interface which allows the user to set a variety of parameters that establish the nature of the information used to calculate the growth vector of, and/or branching capability of hyphal tips in the visualization, and the range over which that information is collected. In essence the user is deciding what the hyphal tips sense and the range over which they sense it.

Six different tropisms can be assigned to the hyphal tips growing in three-dimensional space: (1) negative autotropism, based on the hyphal density field (intensity inversely proportional to distance), with a persistence factor that controls the aversion vector, and the opportunity to rotate the tropic sensor around the hyphal axis; (2) secondary long range autotropism and, if activated, the opportunity to set its impact, the way it attenuates with distance (either directly proportional to the square root of distance or inversely proportional

to the square root of distance), and the opportunity to rotate the tropic sensor around the hyphal axis; (3) tertiary long range autotropism, which attenuates as rapidly as the negative autotropism but can be given a large impact, so the user has the opportunity to set its impact and to rotate the tropic sensor around the hyphal axis; (4) parallel current parallel tropism, which is a galvanotropism (based on electric field produced by the hypha which is parallel to the hyphal long axis) which can orient hyphae in parallel arrays (the field is directional, it corresponds with the growth direction of the hypha; any other hyphal tip which responds to this field will turn to grow in the same direction); (5) parallel current positive/negative tropism, which is a galvanotropism which can bring hyphae together (=positive) or keep them apart (=negative) on the basis of their response to the intensity of the galvanotropic field: this works very similarly to long range autotropism (but, of course, depends on an assumed electrical field, rather than density of hyphae); and (6) gravitropism, which orients hyphae relative to the vertical axis of the user's screen and can be adjusted for angle of response (0–90° positive and negative), sensitivity (range 0 to 1), rotation of the gravitropic sensor around the hyphal axis, and implementation of a hyphal length-dependent gravitropic angle turn which allows the angle of gravitropic response to alter automatically as the mycelium grows.

Growth and branching can be regulated separately and differently from one another: (1) both growth and branching can be controlled by the number of neighbouring tips, the user decides this (the threshold number of tips that effects control) and the size of the neighbourhood within which tips are counted; (2) alternatively, growth and branching can be made dependent on the hyphal density field (=mycelial mass), rather than the number of tips, in the neighbourhood (the density field can be set to depend on hyphal tips, and/or branch points, or all of the mycelium); (3) the growth rate can be set by the user, and the user can set growth rate to be proportional to hyphal length; in this case the user specifies the value of the proportionality coefficient and the maximum specific growth rate; (4) branching will take place at a randomly-chosen position around the periphery of the hypha by default, but the user can set optimal initial branch orientation so that the position of branch emergence will be calculated to be optimal for the tropic vectors acting on the tip at the time of branching; (5) by default there is a 100% probability of branching (subject to other rules set for other features), but the user can determine the probability of branching; (6) maximal branch angle is 180° by default (which effectively means that any angle is acceptable), but the user can set this to any lesser angle of choice; and (7) limits can be set to the age of the hyphal tip and/or length of the hyphal segment, to decide conditions under which growth and/or branching will be halted.

The program is written in Java™ and displayed as a Java™ three-dimensional visualization with which the user can interact in a number of ways. (1) The whole visualization can be rotated around vertical and horizontal axes, and the scale of the display and position of the point of view are controllable by the user. The mycelium or structure visualized can also be displayed as a slice (useful to see internal structure) across *x*, *y* and *z* planes. Thickness of the slice, position and rotation are set interactively by the experimenter. (2) Visualizations as displayed on screen can be saved as images (in JPEG format, and accompanied by TXT files listing the parameter settings), but also the data that produces the visualization can be saved (in XML format) and can subsequently be reloaded into the program for further examination, or for continuation. (3) There are two ways to generate animations with the Neighbour-Sensing program. One is to activate an animation robot that records use of the parameter controls as the user modifies the visualization by manual interaction. This saves a record of the parameter changes made and allows the visualization to be repeated at a later date with exactly the same timing and sequence of parameter changes. However, each time the robot is run a new visualization is created with a new population of hyphal tips, so there will be some ‘natural variation’. The combination of a pre-saved file of parameter settings and an animation robot file of parameter settings is analogous to a living organism’s combination of genome and developmental programme. The second animation technique is to use the Neighbour-Sensing program to generate a series of frames for a digital movie. The frames can then be used by a suitable graphics program to create an AVI-format digital video. This approach is simply a digital video record of one particular visualization, but the AVI-file is more portable, being independent of the Neighbour-Sensing program.

RESULTS

Experiments can be done with the Neighbour-Sensing model by changing the parameters that the simulation uses in its mathematical computations in order to see the effects of those parameters on growth of the fungus on screen. The basic visualization provided by the Neighbour-Sensing model is sufficiently realistic for systematic variation of the parameters to enable detailed analysis of the influence of the different tropisms on hyphal patterning. Simulations can be paused, parameters changed, and the simulation then resumed so that sequential change in (potentially several) parameter sets can be studied. Obviously, with the many parameters open for manipulation in the program there are numerous potential combinations of this sort and what follows in this report is a record of just a few such experiments, illustrated with images of the visualizations generated.

Figs 1A–C show the effects of varying the autotropism setting. Fig. 1A shows a visualization in which no autotropism is assumed, but branching is given a probability of 40% and occurs only when there are fewer than three tips within a radius of 20 distance units (growth only occurs when there are fewer than 15 tips within that radius). Fig. 1B assumes 50% negative autotropism and Fig. 1C, 10% negative autotropism, although all other parameters were unchanged. 10% negative autotropism seems to produce the most realistic mycelial shapes and was the value used in most of the subsequent examples shown. Figs 1D–E illustrate growth patterns produced with different levels of control over the probability of branching, but with the same growth rules: Fig. 1D, branch only when fewer than two tips within a radius of 20 distance units, and Fig. 1E branch only when fewer than eight tips within that radius, all other parameters being identical.

Introducing a limitation on the growth of tips modifies this colony morphology further, resulting in a structure of intermediate density (Fig. 1F, growth only when fewer than 15 tips within the 20 unit radius). However, if this parameter is implemented its value must be larger than that of the branching threshold parameter for a viable, growing mycelium to result. Interestingly, a similar effect to decreasing the threshold for preventing branching and growth can be achieved also by increasing the radius that defines ‘neighbouring tips’. In this scenario, a sparser structure is produced with longer segments of hyphae before branching is initiated (Fig. 1G; neighbourhood increased to 40 unit radius, compared with the 20 units used in earlier visualizations).

By switching between parameter sets like those described above, it is possible to produce more complex structures. For the visualization shown in Fig. 1H, three stages were employed: first, a parameter set was chosen that produces a dense mycelium, and operated for 100 time units; second, the growth threshold and the size of the radius defining the neighbouring tips were adjusted so that only a few tips continued growth. Furthermore, the probability of branching was reduced to a value close to zero. These settings were operated for 200 time units. Finally, a parameter set that produces a dense globular outgrowth of tips was implemented (for 50 time units). Note that the definition of neighbouring tips is kept large in this parameter set so that tips in the original ‘parent’ mycelium do not resume growth.

Most parameter settings generate spherical colonies, and that includes a setting in which all controls are removed and growth and branching depend on randomized decisions. In other words, the basic spherical (circular in projection) morphology of the fungal colony arises without the need for global control of that morphology. Evidently ‘circularity’ of the fungal colony is not a special attribute, but a natural outcome of the fundamental exploratory filamentous growth mode.

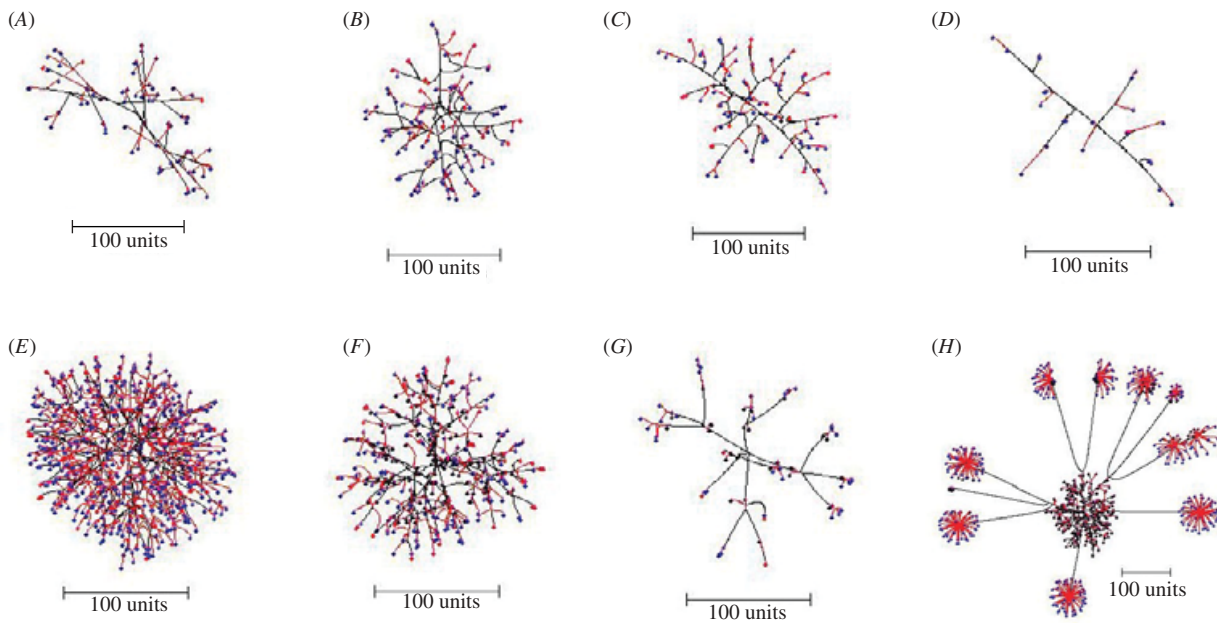


Fig. 1. Hyphal growth patterns in Neighbour-Sensing visualizations produced by specific changes in growth parameters. (A) No autotropism assumed, but branching probability = 40% and occurs only when there are fewer than three tips within a radius of 20 distance units (growth only occurs when there are fewer than 15 tips within that radius). (B) 50% negative autotropism assumed. (C) 10% negative autotropism assumed. (D) Branch only when fewer than two tips within a radius of 20 distance units. (E) Branch only when fewer than eight tips within that radius (parameters not specified were identical to 1C). (F) Grow only when fewer than 15 tips within the 20 unit radius. (G) Neighbourhood radius increased to 40 units. (H) By pausing the visualization and switching between parameter sets like those described above, it is possible to produce more complex structures. For the visualization shown in Fig. 1H, three stages were employed: first, a parameter set was chosen that produces a dense mycelium, and operated for 100 time units; second, the growth threshold and the size of the radius defining the neighbouring tips were adjusted so that only a few tips continued growth, and probability of branching reduced to a value close to zero (these settings were operated for 200 time units); finally, a parameter set that produces a dense globular outgrowth of tips was implemented for 50 time units. In all these figures the small coloured circles at the ends of branches are flags that identify the position of the apex and are colour-coded red for non-growing and blue for growing tips in this iteration of the algorithm. Colour of a hyphal segment in Figs 1–6 depends on the number of growing tips the segment supports, from black (supporting many tips) to red (one tip). Alternative coding (Figs 7–8) is based on distance from the start point (effectively hyphal age); green segments are close to the initial point (= old), and colour varies through magenta, pink and red for distant (= young) segments.

However, the program does not limit us to spherical end-points. A thin filament (Fig. 2A) can be formed by setting the parameters that prevent growth and branching to high thresholds (i.e. the growth and branching of tips is made highly probable), but then limiting the time for which the tips can grow and branch. There are two ways to limit the length of branches – first, by limiting the time for which they grow, and second, by limiting the length to which the segments grow. Both have the same effect. To create a number of tips from where the filament can extend any parameter set can be used that generates reasonably large numbers of tips per time unit. A more prolifically branched filament can be produced (Fig. 2B) by increasing the threshold for preventing branching and growth (i.e. increasing the density of branches) and by allowing the tips to branch and grow for longer. The branching probability can also be increased to accentuate the effect. Increasing the time that the initial parameter set is run at the start, and then switching to a thin filament parameter set can

produce a globular structure with thin ‘exploratory’ filaments emanating from it (Fig. 2C).

Implementing the density field hypothesis for branching regulation represents a slightly different way of calculating the density of tips in the locality. The main practical difference between this form of computation and that in the examples discussed above is that when the density field hypothesis is used, local differentiation becomes difficult as the regulation applies to the whole mycelium. For instance, the structure illustrated in Fig. 1H would be impossible using this method, as it cannot prevent growth and branching in the ‘parent’ mycelium while allowing it in the ‘daughters’. Thus, structures are produced that are uniformly distributed with branches and most branching appears to be dichotomous (it is not strictly dichotomous because of the way the program manages branching). Fig. 3 shows three examples in which the density field threshold for branching was varied to produce mycelia with different morphologies.

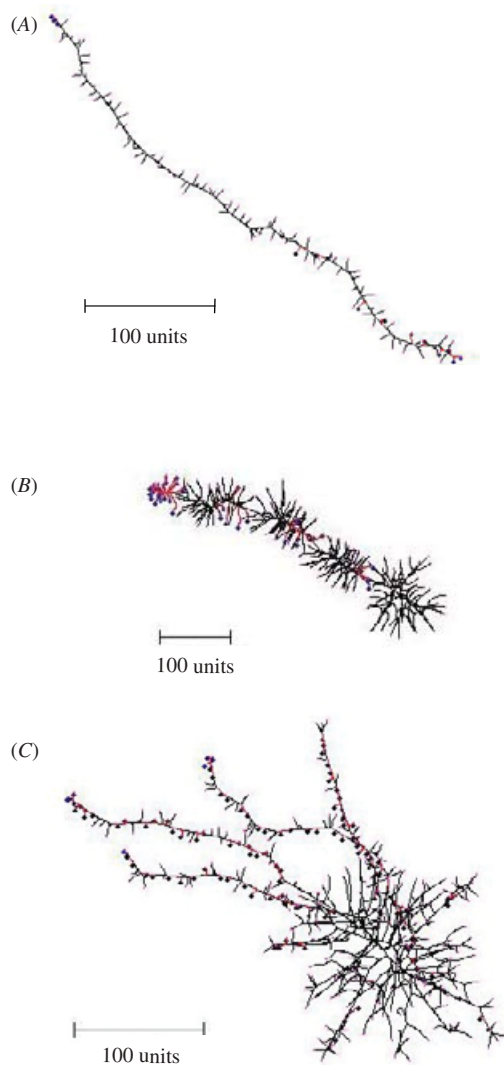


Fig. 2. (A) A thin, sparsely branched filament results when growth and branching limits are set to high thresholds and the time for which the tips can grow and branch is limited. (B) Relaxing these limits results in a more prolifically-branched filament. (C) A globular structure with thin 'exploratory' filaments emanating from it is produced by switching to a thin filament parameter set after a period of normal growth.

If negative autotropism is set to zero at the beginning of the simulation (switching this parameter to zero during a simulation produces different results) an interesting growth process can be seen. This can be done with both methods of branching regulation, but the density field hypothesis is supposed in the examples shown here. The interesting feature of the growth of these mycelia is that they grow in one plane at a time. That is to say, a straight, single hypha grows first with many dormant tips along it; then branches grow perpendicularly to produce a two-dimensional disc-type structure; and finally more branches grow out perpendicularly from that to make a three-dimensional structure. If a relatively high density field threshold is used, an ellipsoidal morphology is produced (Fig. 4A). If the density field threshold is reduced, the result is a rod-like

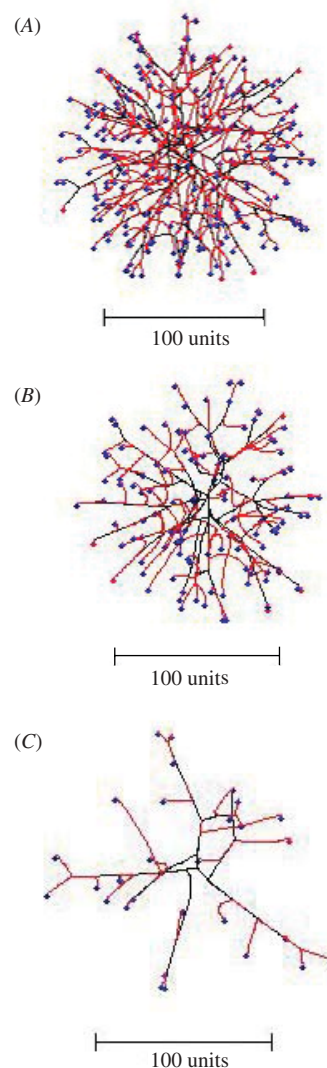


Fig. 3. Three examples showing effect of variation in the hyphal density field. (A) branch if field is less than 0.1. (B) branch if field is less than 0.05. (C) branch if field is less than 0.01.

structure (Fig. 4B). Again, switching between parameter sets in the course of a simulation generates interesting compound morphologies. For Fig. 4C, three parameter sets were used: first, negative autotropism was set to zero and the density field hypothesis supposed, with the threshold for branching set reasonably high (i.e. branching likely), this produced a short, straight hypha with many (dormant) tips in 90 time units; second, once the tips on the hypha began to extend perpendicularly, the branching threshold and probability were lowered so that long branches grew for 110 time units; finally, the branching threshold and probability were raised to very high values and the tip growth was limited to 25 time units, this caused the dense branching around the growing tips at the periphery. For the structure shown in Fig. 4D, an ellipsoid mycelium, as in Fig. 4A, was grown initially for 200 time units. Then the parameters were switched to a set that produced

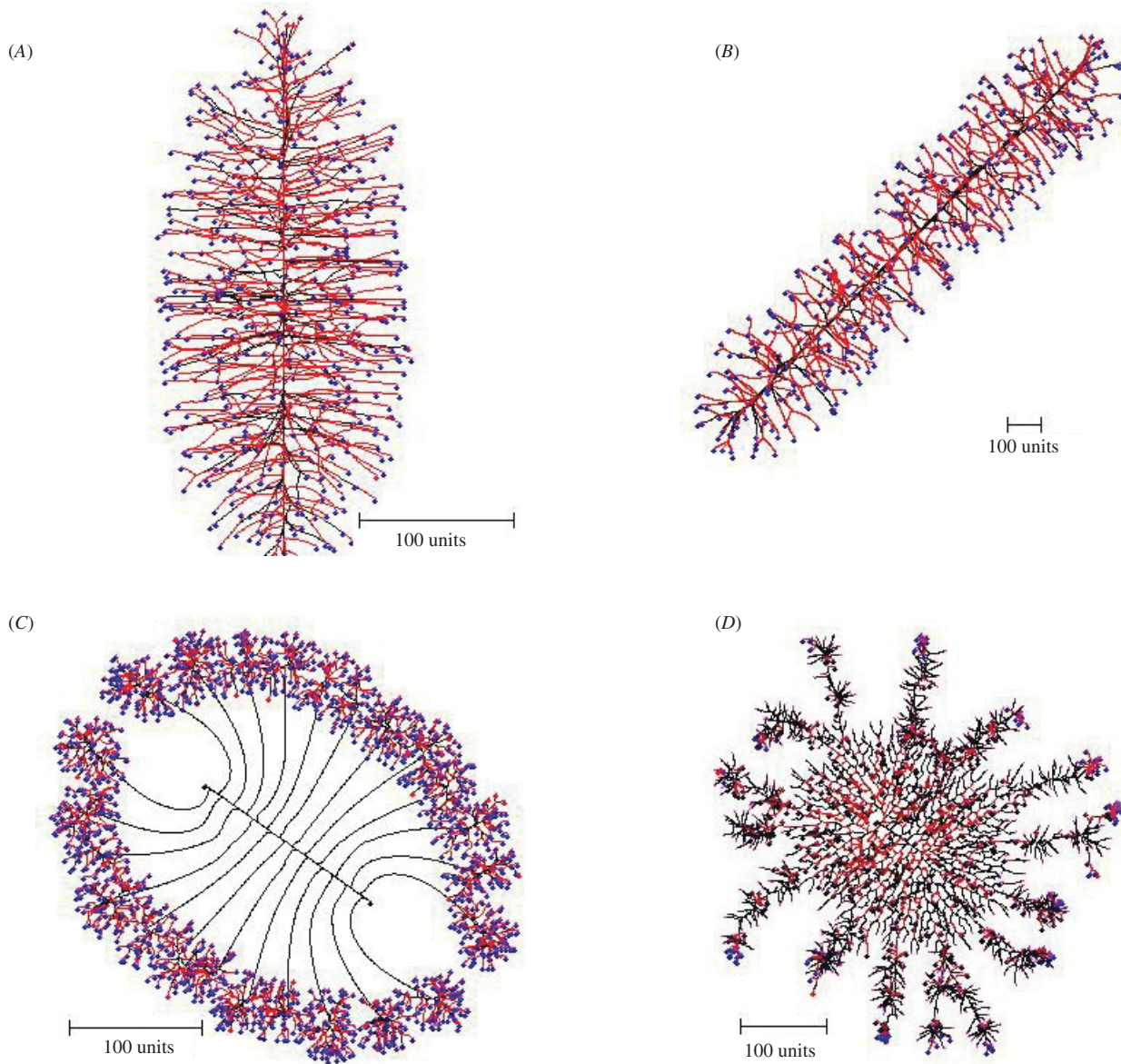


Fig. 4. Controlling morphology with the branching threshold of the hyphal density field. (A) Effect of a relatively high density field threshold that allows branching if field is less than 0.1. (B) Response to a lower field threshold: branch if field is less than 0.005. (C) Results of three consecutive parameter sets featuring branching threshold settings that were first high (0.1), then much lower (0.005), and finally very high (0.5). (D) Another example of parameter switching, the parameters that produced 4A being followed by those that produced 2B.

densely branched filaments (as in Fig. 2B) for a further 100 time units.

When gravitropism is implemented a vector is added to each hyphal tip corresponding to the angle of gravitropism set by the user and for positive angles the tips are constrained to grow upwards in the user's field of view. Again we would emphasize that although we describe this as gravitropism, the mathematical model employs an abstract definition independent of mechanism. This is a vertical orientation field which could equally well be generated by incident illumination or a chemical gradient.

If the angle of negative gravitropism is set to -45° , a cone-shaped structure is produced (Fig. 5A), but a slice through the centre of this shows that it is a hollow

cup-shaped structure rather than a solid cone (Fig. 5B). This is a consequence of negative autotropism being implemented as well, which has a stronger effect in the crowded central region and forces the new tips to grow at 45° away from the central axis. This observation of a structure with similarities to a cup-fungus fruit body suggests that a combination of relatively simple tropisms may be able to generate simulations of other fungal fruit bodies.

By implementing gradual rotational adjustment of the gravitropic angle in a manner that is dependent on branch length it is possible to generate smoothly-curved structures. In the example shown in Fig. 5C, the angle of gravitropism was started at 90° and when the length of each branch reached 100 length units the

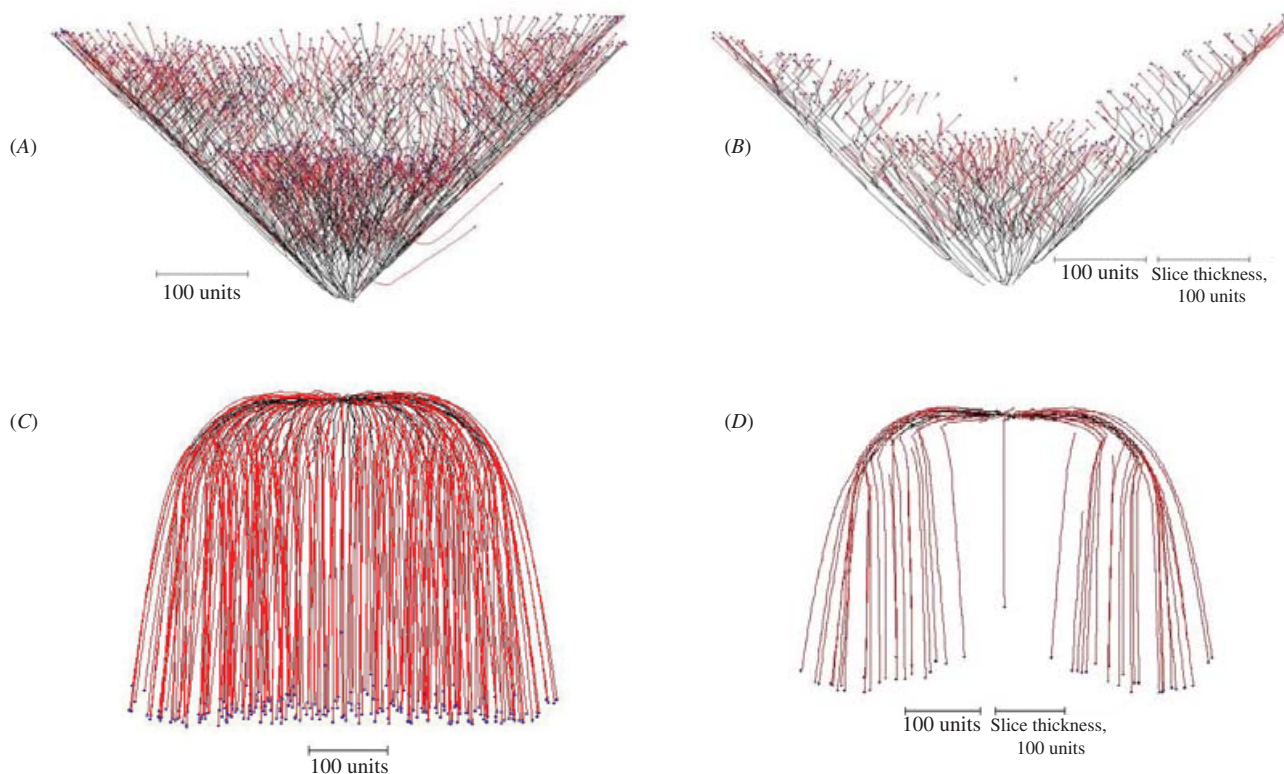


Fig. 5. Implementing the gravitropic response. (A) Setting the angle of gravitropism to -45° produces a cone-shaped structure. (B) A slice through the centre of the cone shows that it is a hollow cup-shape; this is a consequence of negative autotropism, which has a stronger effect in the crowded central region and forces the new tips to grow away from the central axis. (C) Implementing root-distance-dependent gravitropic angle turn gradually changes the angle of gravitropism from one value to another over the course of a defined distance between the tips and their ‘roots’ (equivalent to branch length). In this example, the angle of gravitropism starts at 90° and when the length of the branches reached 100 length units the angle of gravitropism was gradually turned towards 180° , reaching this value when the branch length was 500 length units. (D) A slice through the centre of 5C shows that the negative autotropism, which was also implemented, has forced the growing tips away from each other as they grew towards the bottom of the structure.

angle of (positive) gravitropism was gradually turned towards 180° , reaching this value when the branch length was 500 length units. A slice through the centre of this visualization (Fig. 5D) shows that the hyphal tips were forced away from each other and towards the outer and bottom margins of the structure because negative autotropism was also implemented.

For the structure shown in Fig. 6, a long-range positive autotropism was implemented as well as negative autotropism and negative gravitropism (-45°). Whereas the strength of the negative autotropism vector is quite localised because it attenuates at a rate inversely proportional to the square of distance, the long-range positive autotropism vector is effective over longer distances, being inversely proportional to the square root of the distance. In this example, the mycelium developed as it would without the long-range positive autotropism to form the basal part of the structure, until the tips reached a threshold distance from the main bulk of the mycelium when they are directed back towards each other and a closed structure results.

Fig. 7 illustrates the ‘development’ of a simulated mushroom primordium. For the first 100 time units a

90° gravitropism was imposed to create a flat colony (Fig. 7A); for the next 200 time units a gradual change of plagiogravitropism to a negative gravitropism forms a cup-shape (Fig. 7B). Subsequent increase in the impact of the long distance positive autotropism forces the cup to close; and then reduction in impact of this factor restores the vertical growth, forming a bottle-shaped stem (Fig. 7C). Later changes of long distance autotropic and (positive) gravitropic parameters cause the community of hyphal tips to cascade down the outside of the stem, forming something resembling a mushroom cap (Figs 7D–E). It is especially noteworthy in these figures, especially the developmental sequence illustrated in Fig. 7, that the simulations pass through intermediate shapes that are similar to the fruit bodies of other (non-mushroom) fungi; such as the open more-or-less saucer-shaped or cup-like apothecia of discomycete *Ascomycota* (Figs 5A–B, 7B), the closed cleistothecial ascoma or hypogeous fruit body (Fig. 6), and the perithecial flask-shaped or bottle-like ascoma of pyrenomycete *Ascomycota* (Fig. 7C).

Fungi are able to form several linear structures (strands, cords, rhizomorphs, mushroom stems) that consist of many hyphae growing in parallel in the same

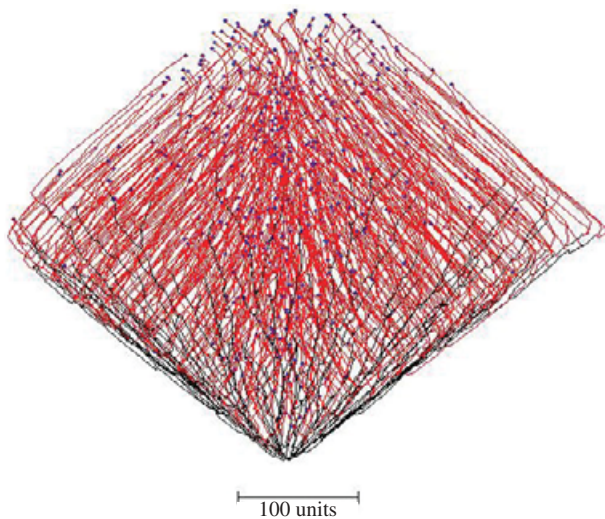


Fig. 6. Combining long-range positive autotropism, negative autotropism and negative gravitropism (-45°). The mycelium grew from the bottom of the figure and developed as a conical structure like Fig. 5A until the tips exceeded the threshold distance from the mycelium when they were directed back towards each other by the long-range positive autotropism. A closed structure results.

direction. Models based only on combinations of negative and positive autotropisms cannot effectively simulate the morphogenesis of such structures because strong positive autotropism (needed to bring the hyphae together) tends to turn the hyphae towards the centre of the developing cybermycelium, and because approaching hyphae have no reason to turn to grow in the same direction. The trajectory of a hyphal tip that is approaching another hypha under the influence of an autotropism strongly depends on the angle of approach. An acute approach angle may cause the approaching hyphal tip to curl around its target in a spiral; an obtuse angle results in the approaching tip 'orbiting' its target aimlessly.

To form linear structures the vector field must have a directional element running parallel to the direction of the linear structure we wish the cyberhyphae to create. In Fig. 7 this purpose was served by gravitropism. An alternative orientation field capable of giving rise to parallel structures is a galvanotropism. From the literature it is evident that bacteria and fungi alike exhibit tropisms to electric fields and currents. Differentially-distributed ion pumps produce ion currents that leave the growing hyphal apex and re-enter the hypha at more basal regions. Hence, at least in some regions the lines of force of the corresponding electric field may be close to parallel to the hyphal axis and able to flow in the surface fluids that commonly surround hyphae in nature. Such a field has the directionality that is needed and can be used for orientation of any approaching hyphal tips. Because the lines of force of the field from each hypha are oriented in the same direction, the shared field of any linear aggregate

structure formed in response to such a field can be much stronger than that generated by a single hypha. Consequently, hyphal recruitment to such a developing aggregate will be a self-accelerating process. We wish to stress that although an electric field seems a likely candidate for this particular tropism (and we refer to it as a galvanotropism), the mathematical model employs an abstract definition of the orientation field which is not dependent on any particular mechanism of generation and/or perception. Other mechanistic hypotheses are not excluded providing they can generate a directional field parallel to the hyphal long axis.

The specific features of this galvanotropism as implemented in the program result from the assumption that each hyphal segment, short enough to be considered as a straight line, forms an orientation field. This field is directed toward the end that is closer to the segment's hyphal tip and is parallel to the hyphal long axis. The absolute value of the field at any given point is inversely proportional to the shortest distance from that point to the segment generating the field. The total field of a mycelium perceived at any given point is a vector sum of the fields generated by all such mycelial segments. Implementing this feature is sufficient to enable the Neighbour-Sensing model to form mushroom-like shapes in a different way from Fig. 7. The outcome of this strategy is illustrated in Fig. 8, where the parallel galvanotropism was used to create an organized structure similar to the developing mushroom stem. Subsequent implementation of a positive gravitropism formed a mushroom cap-like structure.

DISCUSSION

A great deal remains to be done with the Neighbour-Sensing program and we invite assistance with this. To this end are willing to share the program with colleagues who may be interested (contact the corresponding author). Our immediate plans include systematic investigation of simulations of fungal colonies on solid media, pellet formation in liquid media, development of statistical assessment of similarity between simulated and *in vivo* growth and branching patterns, and introduction of several cybermycelia into the visualizations so that hyphal interactions can be simulated.

However, the experiments described above have revealed a fascinating feature of the 'crowd behaviour' of fungal hyphal tips, which is that the shapes of complex fungal fruit bodies can be simulated by applying the same regulatory functions to every one of the growth points active in a structure at any specific time. All of the parameter sets that generate shapes reminiscent of fungal fruit bodies feature an organized series of changes in parameter settings applied to *all* of the hyphal tips in the simulation. No localized regulation is necessary. No global control of fruit body geometry is necessary. The shape of the fruit body

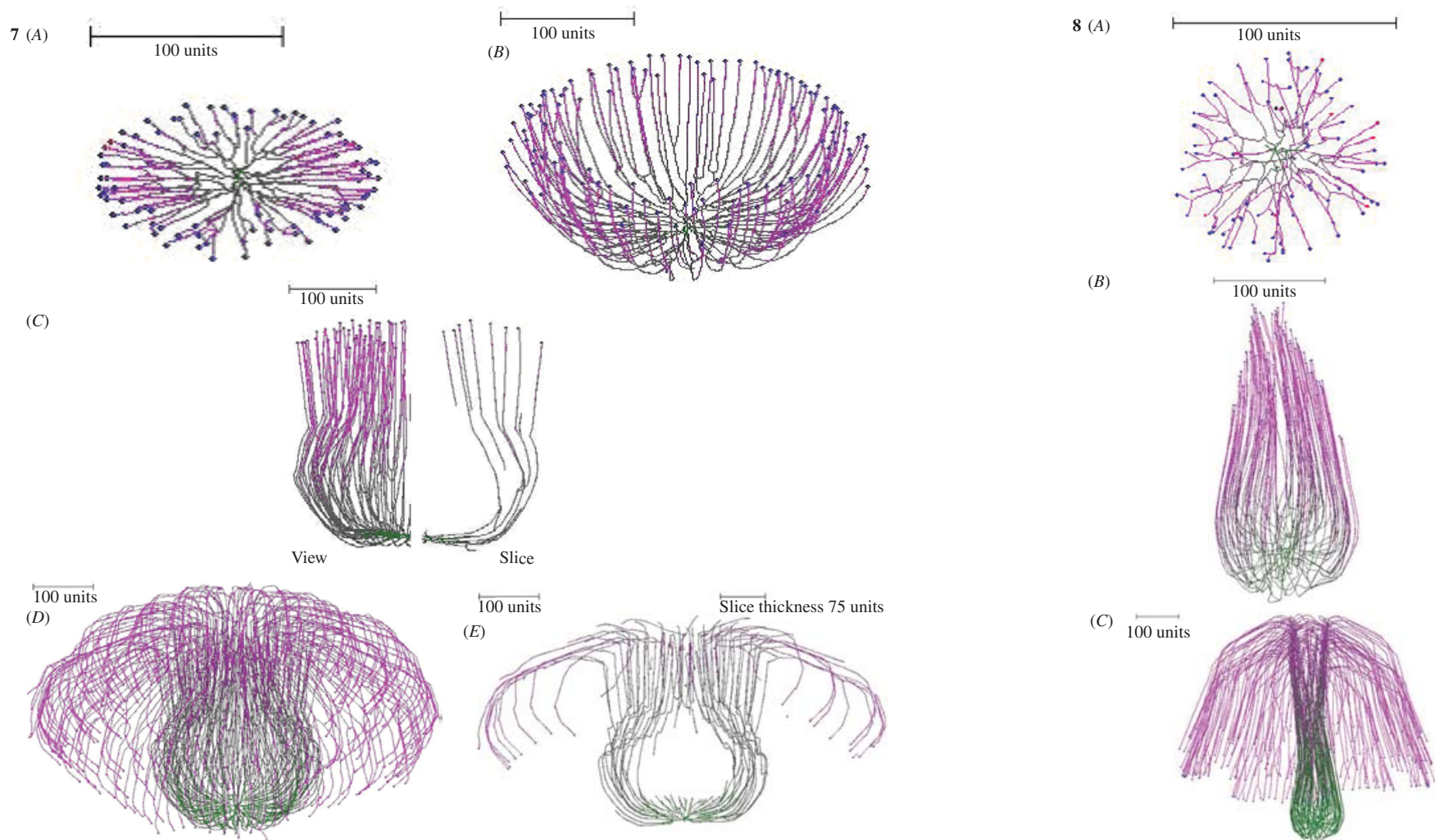


Fig. 7. Successive stages in ‘development’ of a simulated mushroom primordium.

Fig. 8. Another simulation of a mushroom primordium. (A) A spherical colony was first grown for 76 time units. (B) This was converted into an organized structure, similar to the developing mushroom stem by applying the parallel galvanotropism for 250 time units. (C) Subsequent application of a positive gravitropic reaction (as used in Fig. 7D) formed a cap-like structure (1000 time units). Long range autotropism was not used. Parallel tropism and current related positive galvanotropism were set to 0.1 after the age of the developing spherical colony reached 76 units. Tropism persistence factor was 0.1, hyphal density field hypothesis was supposed, with a branching threshold of 0.06 field units, field based self-avoidance reaction was supposed, and the field was generated by all of the mycelium.

emerges from the concerted response of the entire population of hyphal tips, in the same way, to the same signals. In the real biological system such morphogenetic programmes could be based on internal 'clocks' of some sort that synchronize behaviour across a developing structure on the basis of time elapsed since some initiating event. This is the most significant observation of our initial series of model experiments.

ACKNOWLEDGEMENTS

We thank Mark Fricker, Peter Darrah and Sarah Watkinson (Department of Plant Sciences, University of Oxford) for many helpful discussions and Mark Fricker especially for helpful comments on a draft of this manuscript. The staff of the High Performance Computing Team at Manchester Computing is thanked for their assistance and welcoming attitude. A.M. was an Honorary Visiting Research Fellow in the School of Biological Sciences in the University of Manchester while this work was carried out. L.J.M. thanks the British Mycological Society for the award of a Bursary that enabled his contribution to this paper.

REFERENCES

- Hutchinson, S. A., Sharma, P., Clarke, K. R. & MacDonald, I. (1980) Control of hyphal orientation in colonies of *Mucor hiemalis*. *Transactions of the British Mycological Society* **75**: 177–191.
- Lever, M. C., Robertson, B. E. M., Buchan, A. D. B., Miller, P. F. P., Gooday, G. W. & Gow, N. A. R. (1994) pH and Ca²⁺ dependent galvanotropism of filamentous fungi – implications and mechanisms. *Mycological Research* **98**: 301–306.
- Matsuura, S. & Miyazima, S. (1993) Colony of the fungus *Aspergillus oryzae* and self-affine fractal geometry of growth fronts. *Fractals* **1**: 11–19.
- Momany, M. (2002) Polarity in filamentous fungi: establishment, maintenance and new axes. *Current Opinion in Microbiology* **5**: 580–585.
- Moore, D. (1991) Perception and response to gravity in higher fungi – a critical appraisal. *New Phytologist* **117**: 3–23.
- Obert, M., Pfeifer, P. & Sernetz, M. (1990) Microbial growth patterns described by fractal geometry. *Journal of Bacteriology* **172**: 1180–1185.
- Olsson, S. (2002) Colonial growth of fungi. In *The Mycota*. Vol. 8. *Biology of the Fungal Cell* (R. J. Howard & N. A. R. Gow, eds): 125–141. Springer-Verlag, Berlin.
- Ott, A., Spencer-Phillips, P. T. N., Willey, N. & Johnston, M. A. (2003) Topology: a novel method to describe branching patterns in *Peronospora viciae* colonies. *Mycological Research* **107**: 1123–1131.
- Pirt, S. J. (1967) A kinetic study of the mode of growth surface colonies of bacteria and fungi. *Journal of General Microbiology* **47**: 181–197.
- Prosser, J. I. & Trinci, A. P. J. (1979) A model for hyphal growth and branching. *Journal of General Microbiology* **111**: 153–164.
- Ritz, K. & Crawford, J. (1990) Quantification of the fractal nature of colonies of *Trichoderma viride*. *Mycological Research* **94**: 1138–1152.
- Robinson, P. M. (1973a) Chemotropism in fungi. *Transactions of the British Mycological Society* **61**: 303–313.
- Robinson, P. M. (1973b) Autotropism in fungal spores and hyphae. *Botanical Review* **39**: 367–384.
- Steele, G. C. & Trinci, A. P. J. (1975) The extension zone of mycelial hyphae. *New Phytologist* **75**: 583–587.
- Trinci, A. P. J. (1971) Influence of the peripheral growth zone on the radial growth rate of fungal colonies. *Journal of General Microbiology* **67**: 325–344.
- Trinci, A. P. J. (1984) Regulation of hyphal branching and hyphal orientation. In *Ecology and Physiology of the Fungal Mycelium* (D. H. Jennings & A. D. M. Rayner, eds): 23–52. Cambridge University Press, Cambridge, UK.
- Trinci, A. P. J., Saunders, P. T., Gosrani, R. & Campbell, K. A. S. (1979) Spiral growth of mycelial and reproductive hyphae. *Transactions of the British Mycological Society* **73**: 283–292.
- Trinci, A. P. J., Wiebe, M. G. & Robson, G. D. (1994) The mycelium as an integrated entity. In *The Mycota*. Vol. 1. *Growth, Differentiation and Sexuality* (J. G. H. Wessels & F. Meinhardt, eds): 175–193. Springer-Verlag, Berlin.
- Viniegra-Gonzalez, G., Saucedo-Castaneda, G., Lopez-Isunza, F. & Favela-Torres, E. (1993) Symmetric branching model for the kinetics of mycelial growth. *Biotechnology and Bioengineering* **42**: 1–10.
- Yang, H., King, R., Reichl, U. & Gilles, E. D. (1992) Mathematical model for apical growth, septation, and branching of mycelial microorganisms. *Biotechnology and Bioengineering* **39**: 49–58.

Corresponding Editor: N. P. Money